DYNAMICS OF A HYDRODYNAMIC SUPPORTED SCREW PUMP ROTOR

Joachim Thurner[1], Peter F. Pelz[1], Frank Holz[2]

[1]Technische Universität Darmstadt
Chair of Fluid Systems Technology
Magdalenenstraße 4, 64289 Darmstadt, Germany
joachim.thurner@fst.tu-darmstadt.de
peter.pelz@fst.tu-darmstadt.de

[2]Leistritz Pumpen GmbH
Marktgrafenstraße 29-39, 90459 Nürnberg, Germany
fholz@leistritz.com

Abstract

Results of a hydrodynamic 2D lubrication model and a 1D contact force model are used for a transient rigid body simulation of the idle spindle motion. The calculated displacement results are compared to experimental results. It turns out, that structural bending caused by pressure difference is overlayed to rigid body displacement.

1. Introduction

Three-spindle screw pumps are kinematic pulsation free displacement pumps. The sidewise idle spindles are driven by engagement of the center drive spindle. The spindles are supported by an oil film within the gap between the spindle surface and the housing. In unpropitious operation points of low rotating speed, low viscosity and high pressure, contact and possible abrasion between idle spindle and housing may occur. This operation limit is determined experimentally by the pump manufacturer. Thus development of a new series is a high financial risk for the producers. *The aim of the research project is to determine the operation limit by physical modeling.*

2. Experimental Set Up

For validation purposes within the research project the displacement of the idle spindle towards the housing wall is detected by a set of inductive displacement sensors (Fig. 1).

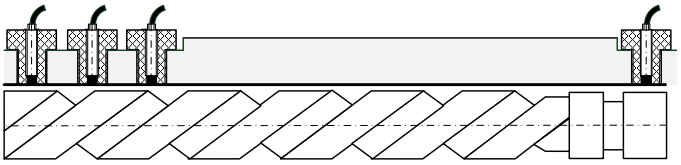

Fig. 1: Axial sensor positions.

Due to the suction-side chamber profile of the idle spindle and the saturation of the measurement range, a valid 360° turn angle signal of the spindle displacement with one sensor is impossible. The problem is solved by a cascade of 3 sensors, corresponding in their axial distance with the thread pitch of the screws. The valid sensor signal is chosen by turn angle information.

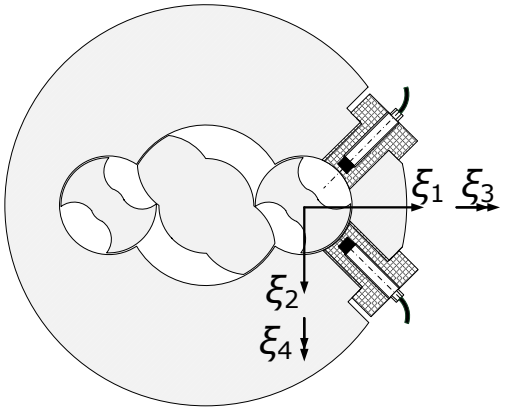

Fig. 2: Peripheral sensor positions.

For horizontal and vertical displacement measurement, the sensor system is arranged in two

perpendicular planes. By doing so, the complete rigid body motion (lateral and angular displacement except axial displacement) is detectable. Due to the fact that a changeless absolute calibration of the center of the screw to the center of the housing is impossible, displacement curves are related to an initial operation point, recorded in the same test series than the other operation points.

3. Hydrodynamic Model

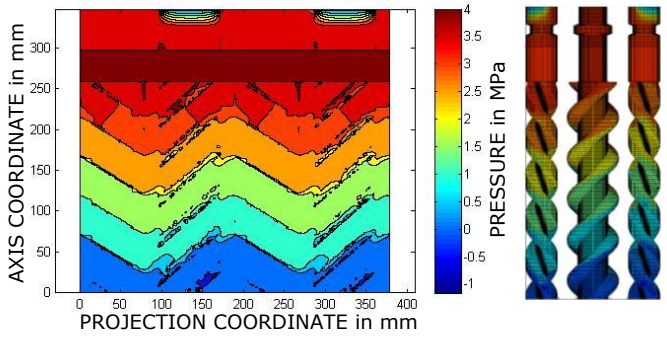

Fig. 3: Hydrodynamic model of the pump. Pressure distribution at a pressure difference of 39 bar, a shaft speed of 3000 rpm und a dynamic viscosity of 5 mPas.

The displacement measurement results are compared with calculation results based on a physical model for the hydro- and rotor dynamics. For the simulation model the hydrodynamics of the pump is represented by a two-dimensional lubrication model [1][2]. Fig. 3 shows the resulting pressure distribution of an example operation point of difference pressure 39 bar, shaft speed 3000 rpm and a dynamic viscosity μ of 5 mPas. To solve the Reynolds lubrication equation, the three spindles are considered to be unwound. By doing so undercuts are treated by simplifying the geometry. Leakage between spindles are not taking into account, which is reasonable for having rotor dynamics in focus and not the volumetric efficiency of the pump.

We take advantage of the linearity of the Reynolds equation of lubrication theory [4]. Due to the linearity in pressure p and speed, the fundamental solutions for different operation conditions are superposed in a linear combination. The Reynolds equation for static pressure p

$$\nabla \cdot \left(\frac{h^3}{\mu} \nabla p \right) = 6\nabla \cdot (h\vec{U}_1 + h\vec{U}_2) + 12 \frac{\partial h}{\partial t},$$

and projection of the shear stress vector on the spindle surface

$$\vec{\tau} = \frac{\mu}{h}(\vec{U}_2 - \vec{U}_1) - \frac{h}{2}\nabla p$$

gives the stress vector $\vec{t}$ of the spindle surface as

$$\vec{t} = \vec{\tau} - p\vec{n}.$$

All physical quantities are linear functions of pressure difference, spindle wall speed $\vec{U}_1$, opposite wall speed $\vec{U}_2$ and rate of chance of gap height $\partial h / \partial t$ and nonlinear functions of gap with h.

The homogeneous solution is given by the pressure difference Δp and suction pressure p_0 for arbitrary position of the spindle $\vec{\xi} = (\xi_1, \xi_2, \xi_3, \xi_4)$ (see Fig. 2 for the coordinates) in the form

$$p_I = p_I(\Delta\tilde{p} = 1, \vec{\xi}, \varphi)\, \Delta p + p_0.$$

To gain the fundamental solution of the Reynolds equation for the specific geometry only one simulation at a given pressure difference $\Delta\tilde{p}$ and displacement of the spindle has to be performed. Due to the linearity of the differential equation the scaling to the actual pressure is linear.

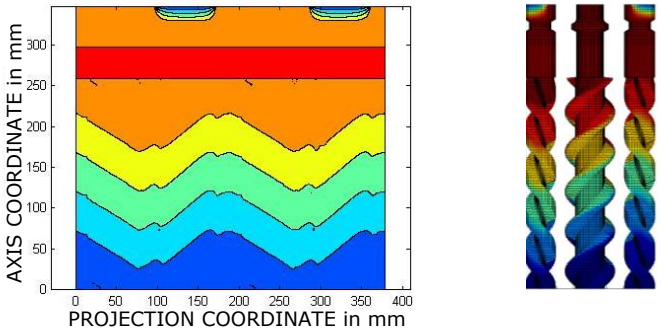

Fig. 4: 1st fundamental solution, influence of the pressure difference.

Figure 4 shows the resulting pressure distribution of the homogenious solution. The stepwise pressure generation from chamber to chamber can be seen. The flow resistance is mainly given by the gaps between the chambers.

The most important inhomogeneous solution results from rotating speed Ω. It may be solved in the same manner:

$$p_{II} = p_2(\tilde{\mu}\tilde{\Omega} = 1, \vec{\xi}, \varphi)\ \mu\Omega$$

For a lateral displaced idle spindle Fig. 5 shows the typical pressure distribution of a journal bearing with a pressure maximum in front and a minimum behind the point of constriction.

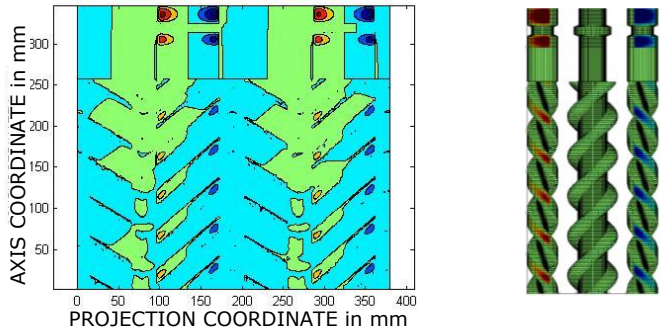

Fig.5: 2nd fundamental solution, influence of rotating speed.

The lateral displacement speeds $\dot{\xi}_1, \dot{\xi}_2$ or cardanic displacement speeds $\dot{\xi}_3, \dot{\xi}_4$ lead to viscous damping forces (torques):

$$p_{III} = \sum_i p_{III}(\tilde{\mu}_i\tilde{\dot{\xi}}_i = 1, \vec{\xi}, \varphi)\ \mu\dot{\xi}_i\ .$$

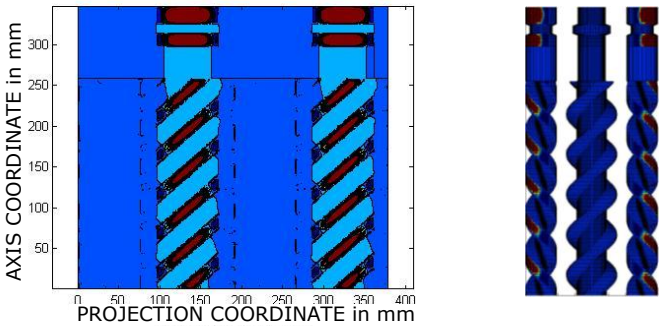

Fig. 6: 3rd fundamental solution, damping due to a lateral displacement.

If the spindle moves towards the wall, the fluid gets squeezed out and a pressure maximum results at this point (see Figure 6 and 7).

By mischance, pressure and other wall stresses are non-linear and coupled functions of translational and cardanic spindle displacement, because Reynolds equation is nonlinear in gap width h. The resulting forces and moments related to the centroid of the spindle are interpolated for all coordinates in polynomial or physical based approaches.

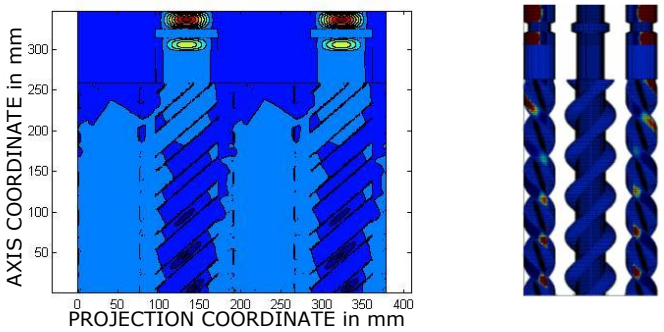

Fig. 7: 3rd fundamental solution, damping due to cardanic movement.

4. Hertz Contact Model

Beside the hydrodynamic forces, the contact between drive and idle spindle are modeled by employing the analytic results of Heinrich Hertz. Based on the analytic results of Hertz for contact between two cylinders, the contact force (per depth) is calculated every cross-sectional area and integrated over the spindle length [5]. Its direction is given by the surface normal of the drive spindle at the contact point (see Fig. 8).

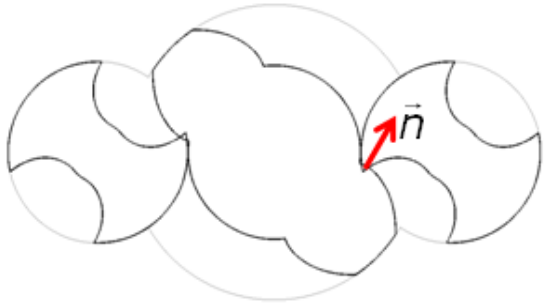

Fig. 8: Hertz contact model.

5. Nonlinear, Transient Simulation of the Rotor Displacement

Interpolations of hydrodynamics and contact are used for transient simulation of the idle spindle motion (Fig. 9).

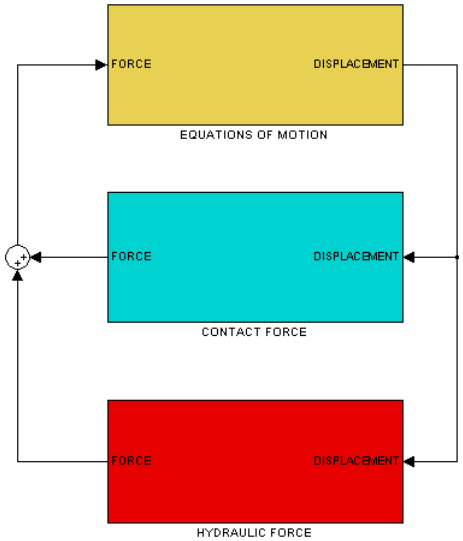

Fig. 9: Block schema of the dynamic simulation model.

6. Results

The experiment is performed pumping oil of only 5 mPas dynamic viscosity at 30°C. The pressure difference was varied up to 40 bar, the rotational speed was varied up to 1500 rpm.

We first were surprised to notice a bending of the spindle as a result of the pressure load on the spindle. This result shown in Fig. 10 was unexpected and seen for the first time since up to now it was common to assume a rigid movement of the spindle within a hydrodynamic supported 3-spindle screw pump. As a result it is not possible to relate displacements at measurement positions to the centroid of idle spindle. Fig. 10 shows the bending line of idle spindle at various pressures relative to the displacement at 5 bar [3].

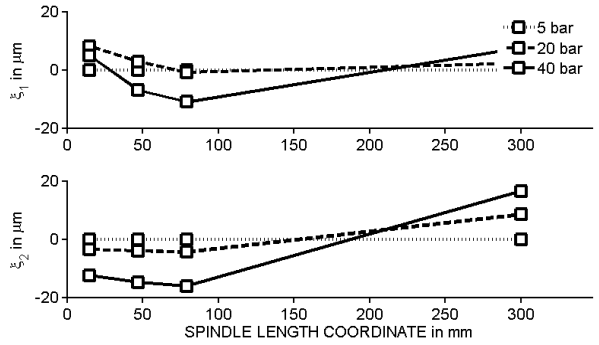

Fig. 10: Bending lines measured at 5, 20 and 40 bar, at 1000 rpm and 5 mPas related to 5 bar.

Under the assumption, the pressure difference is the main cause for elastic bending, a test series with constant pressure difference and variable oil temperature was done. While temperature rises from 30 to 60 °C, dynamic viscosity falls from 5 to 2.5 mPas. It can be seen, that the bending line is much more linear. The spindle displaces likewise a rigid body [3].

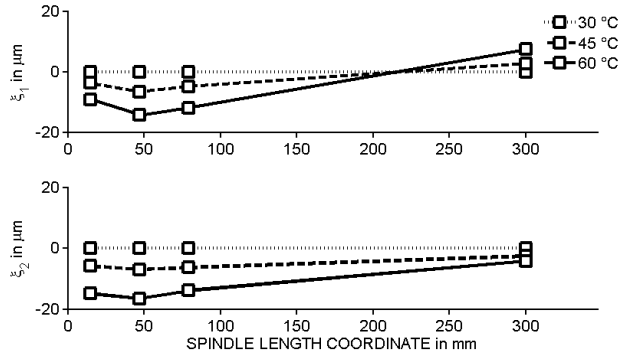

Fig. 11: Bending lines measured at 30 bars and 1000 rpm at temperatures of 30, 45 and 60°C related to 30°C.

Compared with the results of simulation (Fig. 12), at variation of dynamic viscosities the qualitative same displacement can be seen.

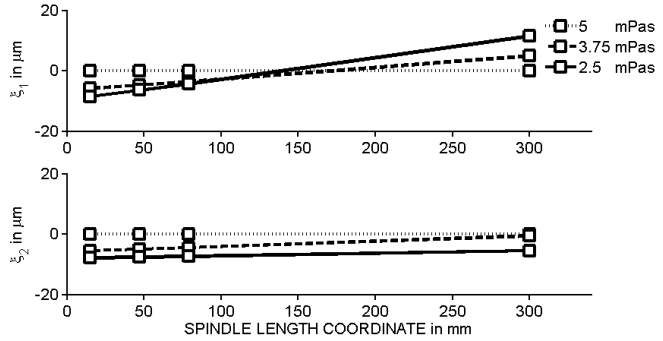

Fig. 12: Bending lines simulated at 30 bar and 1000 rpm at viscosities from 2.5 to 5 mPas related to 5 mPas.

The simulation model is able to reproduce the displacement of the idle screw without usage of any empirical based parameters. Uncertainties of simulation seem to be less significant for the result then the influence of manufacturing tolerances. In future works we will have a closer look on bending aspects.

A linearization of the equations of motion of the idle spindle was done, and positive eigenvalues and thus dynamic instability for operation points of high viscosity and rotating speed at low pressure differences was found. The journal bearing effect leads to dynamic instability, due to the fact the main force reaction is perpendicular to the displacement direction. By now, the effect could not be verified by measurement results.

List of Symbols

p	pressure
h	gap height
t	time
ξ_1, ξ_2	lateral displacement
ξ_3, ξ_4	cardanic displacement
μ	dynamic viscosity
Ω	rotating speed
$\vec{n}$	normal
$\vec{U}_1$	wall speed of spindle
$\vec{U}_2$	opposite wall speed
$\vec{t}$	wall stress vector
$\vec{\tau}$	shear stress vector
$\vec{\xi}$	vector of displacements

References

[1] Bevern, S., Thurner, J., Pelz, P., Holz, F.: Das dynamische Betriebsverhalten von Schrauben-pumpen – ein neuer innovativer Berechnungsansatz, 8. VDI-Fachtagung Schraubenmaschinen 2010

[2] Bevern, S: Spaltströmungen und daraus resultierende Kräfte bei Spindelpumpen, TU Darmstadt, Bachelorarbeit 2009

[3] Rossow, P: Experimentelle Untersuchung der Verlagerung gleitgelagerter Schraubenpumpen-Rotoren, TU Darmstadt, Bachelorarbeit 2011

[4] Spurk, J., Aksel, N.: Strömungslehre, Einführung in die Theorie der Strömungen, 7 Auflage, Springer-Verlag Berlin Heidelberg 2007

[5] Popov, V.: Kontaktmechanik und Reibung, 2 überarbeitete Auflage, Springer-Verlag Heidelberg Berlin 2011

Acknowledgment

We want to thank the employees of Leistritz Pumpen GmbH for their support to our scientific project with their experience, their time and with components.
The presented results were obtained within the research project ZIM KF2529401, funded by budget resources of the Bundesministerium für Wirtschaft und Technologie (BMWi) approved by the Arbeitsgemeinschaft industrieller Forschungs-vereinigungen “Otto von Guericke” e.V. (AiF).